RESEARCH PAPER

Synthesis and characterization of graphene-based nanocomposites with potential use for biomedical applications

Daniele Nuvoli · Valeria Alzari · Roberta Sanna ·
Sergio Scognamillo · Jenny Alongi ·
Giulio Malucelli · Alberto Mariani

Abstract In the present study, graphene-based nanocomposites containing different amounts of nanofiller dispersed into Bis-GMA/tetraethyleneglycol diacrylate (Bis-GMA/TEGDA) polymer matrix have been prepared. In particular, the graphene dispersions, produced at high concentration (up to 6 mg/ml) by simple sonication of graphite in TEGDA monomer, have been used for the direct preparation of nanocomposite copolymers with Bis-GMA. The morphology of the obtained nanocomposites has been investigated as well as their thermal and mechanical properties. SEM analyses have clearly shown that graphene deeply interacts with the polymer matrix, thus resulting in a reinforcing effect on the material as proved by compression and hardness tests; at variance, graphene does not seem to affect the glass transition temperature of the obtained polymer networks.

Keywords Graphene · Nanocomposites ·
Acrylic copolymers · Mechanical properties

D. Nuvoli · V. Alzari · R. Sanna · S. Scognamillo ·
A. Mariani (✉)
Dipartimento di Chimica e Farmacia, Università di
Sassari, Local INSTM Unit, Via Vienna 2, 07100 Sassari,
Italy
e-mail: mariani@uniss.it

J. Alongi · G. Malucelli (✉)
Dipartimento di Scienza Applicata e Tecnologia,
Politecnico di Torino, sede di Alessandria, Local INSTM
Unit, Viale T. Michel 5, 15121 Alessandria, Italy
e-mail: giulio.malucelli@polito.it

Introduction

As far as their use for biomedical applications is concerned, acrylic systems have found great interest. In particular, they have been exploited as pH-sensitive polymers [like poly(acrylic acid), poly(methacrylic acid) or poly(N,N-dialkyl aminoethyl methacrylates], stimuli-responsive hydrogels, drug delivery systems, and dental restorative materials (Aguilar et al. 2007). In particular, the development of resin-based filling composites has revolutionized the field of dentistry over the past 30 years. Compared to dental amalgams, composites possess better esthetic property, have less safety problems and have shown reasonably satisfactory clinic results (Soh et al. 2006). Over the years, the properties and performance of these materials have been improved by modifications in their formulation, such as the use of new organic monomers and fillers (Soh et al. 2006). Since the early 1960s, 2,2′-bis-[4-(methacryloxypropoxy)-phenyl]-propane (Bisphenol A glycerolate dimethacrylate, Bis-GMA) has been widely used as an important dental base monomer, which combines its mechanical characteristics with the advantage of limiting the volumetric shrinkage upon polymerization and enhancing the resin reactivity (Bowen 1962, 1963); however, because of its high viscosity, monomers as triethyleneglycol dimethacrylate (TEGDMA), which are less viscous, are added to the resin for improving the handling features and increasing the double-bond conversion (Bowen 1965). For this reason, 50/50 w/w Bis-GMA/TEGDMA

mixtures are those that are used most for the preparation of dental composites, where the final properties are enhanced by the addition of large amounts of inorganic fillers, such as micro- or nano-sized SiO_2, ZrO_2, Al_2O_3, and silicate glasses (Antonucci and Stansbury 1997; Roberson et al. 2002; Chen et al. 2005). The resins reinforced with bioactive glass, Al_2O_3 or other fillers, have been also used for craniofacial and orthopedic applications like bone implants and prostheses (Ballo et al. 2011; Palussière et al. 2005; Tuusa et al. 2007; Zhao et al. 2009).

Graphene, one of the allotropes of elemental carbon, is a planar monolayer of carbon atoms arranged into a two-dimensional honeycomb lattice with a carbon–carbon bond length of 0.142 nm (Slonczewski and Weiss 1958). It has demonstrated a variety of intriguing properties including high electron mobility at room temperature (250,000 cm^2 V^{-1} s^{-1}) (Novoselov et al. 2004, 2005), exceptional thermal conductivity (5,000 Wm^{-1} K^{-1}) (Balandin et al. 2008) and superior mechanical properties, with a Young's modulus of 1 TPa (Lee et al. 2008). Its potential applications include single molecule gas detection (Schedin et al. 2007; Sofo et al. 2007), transparent conducting electrodes (Wang et al. 2008), energy storage devices such as supercapacitors (Stoller et al. 2008), lithium ion batteries (Yoo et al. 2008), fabrication of transistors (Ponomarenko et al. 2008; Wang et al. 2009), and use in nanocomposite materials with enhanced properties (Stankovich et al. 2006; Kim et al. 2010; Potts et al. 2011).

One of the most effective and promising routes for the bulk production of graphene (and its use for nanocomposite production) is the exfoliation of graphite in a liquid medium to form colloidal suspensions of single or few-layered graphene sheets (Park and Ruoff 2009). Usually, the production by this method involves the synthesis of graphite oxide because it facilitates the exfoliation and the dispersion in polar solvents; however, oxidation results in considerable damaging of graphene electronic structure, which can be only partially restored by reduction processes. As a consequence, the so-obtained "graphene" actually still contains a number of oxidized carbons, and consequently is characterized by properties that differ from those that real graphene may exhibit (Coleman 2013). This drawback, combined with the high number of synthetic steps envisaged by this approach, suggested many researchers to find

easier alternative routes. In particular, Hernandez et al. (2008) succeeded in obtaining graphene sheets by direct graphite exfoliation in N-methylpyrrolidone, with a non-chemical solution phase method, based on the assumption that the energy required to exfoliate graphene is balanced by the solvent-graphene interaction for compounds having a surface energy similar to graphene. At variance to the other methods reported in literature, this synthetic route allows avoiding special apparatuses (Aizawa et al. 1990; Lu et al. 1999; Berger et al. 2006), and any chemical manipulation, which eventually results in defect-containing graphene (Lerf et al. 1998; Boukhvalov and Katsnelson 2008; Li et al. 2008). The development of this method allowed reaching the highest concentrations reported so far in any solvent and to synthesize polymer nanocomposites, with the further advantage of avoiding any solvent to be eventually removed (Nuvoli et al. 2011, 2012; Alzari et al. 2011a, b; Sanna et al. 2012; Scognamillo et al. 2012; Khan et al. 2010, 2011). As far as nanocomposites are concerned, it was assessed that a very small amount of graphene is sufficient to largely improve the resulting mechanical properties (Alzari et al. 2011a, b; Ramanathan et al. 2008; Rafiee et al. 2009; Verdejo et al. 2008).

Furthermore, several studies demonstrated that graphene oxide is potentially cytotoxic (Sasidharan et al. 2011; Sanchez et al. 2012), while graphene obtained by direct exfoliation in liquid media does not seem to be so (Sanchez et al. 2012, Fan et al. 2010, Sasidharan et al. 2012). These findings further justify the use of graphene instead of some of its more or less reduced forms for biomedical applications. More specifically, Fan et al. (2010) showed that graphene/chitosan composite materials have good biologic safety and displayed almost noncytotoxicity (Hailong et al. 2010). Sasidharan et al. (2012) not only demonstrated the biocompatibility of graphene dispersed into a polymer (graphene dispersions on mammalian cells were tested and showed ~ 80 % cell survival) but also its antibacterial properties. Indeed, the microbial growth of *Escherichia coli* and *Bacillus subtilis*, after exposure to the graphene/polymer nanocomposite, showed fewer viable and active bacteria as compared with the exposure to pure polymer or pure graphene dispersions.

In this study we investigated the use of graphene as novel nanofiller in Bis-GMA/TEGDA copolymers, which might be of interest in biomedical applications.

TEGDA has been used instead of TEGDMA because of its superior characteristics as an effective dispersing medium for graphene (Alzari et al. 2011b). However, in order to investigate the real contribution of graphene on the mechanical properties of the polymer matrix, at variance to what happens in commercial formulations, no other filler was added. More specifically, graphene was obtained at high concentration by simply sonicating graphite in TEGDA and the resulting dispersions were used for the direct preparation of nanocomposite copolymers with Bis-GMA. Their morphology and their thermal and mechanical properties have been investigated and correlated with the nanofiller content.

Experimental section

Materials

TEGDA (MW = 302.32, d = 1.11 g cm^{-3}), TEGDMA (MW = 286.32, d = 1.092 g cm^{-3}), Bis-GMA (MW = 512.6, d = 1.161 g cm^{-3}), benzoyl peroxide (BPO, MW = 242.23), and graphite flakes (particle size, +100 mesh) were purchased from Sigma-Aldrich and used as received.

Preparation of graphene dispersions in TEGDA

The procedure used for the preparation of a graphene/TEGDA masterbatch at high concentration is reported by Alzari et al. (2011b). In brief, 5 g of TEGDA were put in a tubular plastic reactor (i.d. 15 mm) and added 5 wt% of graphite flakes; the reactor was placed in an ultrasonic bath (0.55 kW, water temperature ≈ 25 °C) for 24 h. Then, the mixture was centrifuged for 30 min at 4,000 rpm to precipitate unexfoliated graphite flakes and the black liquid-phase containing graphene was recovered.

The graphene concentration, calculated by gravimetry after filtration through polyvinylidene fluoride filters (pore size 0.22 μm), was 6 mg ml^{-1}.

In order to determine the actual graphene content in any diluted dispersion used for the nanocomposites preparation, UV–Vis spectroscopy measurements were performed with a Hitachi U-2010 spectrometer (1 cm cuvette, λ = 660 nm and ε = 436 mL mg^{-1}m^{-1}).

Raman spectra were carried of confirming the presence of graphene. Samples for analyses were prepared by vacuum filtration of dispersions on PVDF filters (pore size 0.22 μm), the spectra were collected with a Bruker Senterra Raman microscope, using an excitation wavelength of 532 nm at 5 mW. The spectra were acquired by averaging 5 acquisitions of 5 s with a 50× objective.

Synthesis of Bis-GMA/TEGDA nanocomposites

Polymer resins were prepared as follows: the graphene masterbatch dispersion in TEGDA was diluted with suitable amounts of this latter liquid monomer for achieving the desired concentration (for the neat resin, pure TEGDA was employed); an appropriate amount of Bis-GMA was added for obtaining a 1:1 w/w mixture, then 1 wt% (referred to the total weight) of BPO was added and the mixture was homogenized. Polymerization was performed in silicone molds (1 × 1 × 0.3 cm^3) at 80 °C for 24 h. For comparative purposes, TEGDA was replaced with TEGDMA, following the same procedure described above.

Characterization techniques

Differential Scanning Calorimetry (DSC) measurements on the PBT and their nanocomposites were performed by means of a Q100 Waters TA Instruments calorimeter, equipped with TA Universal Analysis 2000 software. The surface morphology of the samples was investigated using a scanning electron microscope (SEM, LEO 1450VP). The specimens (0.5 × 0.5 mm^2) were fractured in liquid nitrogen, fixed to conductive adhesive tapes and gold-metallized.

Compression tests, according to ASTM D695, were performed, using a Zwick-Roll Z010 apparatus, equipped with a 5 kN load cell, at 23 ± 2 °C and 50 ± 5 % relative humidity. At least five tests were repeated for each material to have reproducible and significant data. Standard deviation (SD) was always below 5 %.

The surface hardness of the samples was measured according to ASTM D2240 (Shore A) at 23 ± 2 °C and 50 ± 5 % relative humidity. At least one measurement at each of five different points distributed over the specimen was performed, using the median of

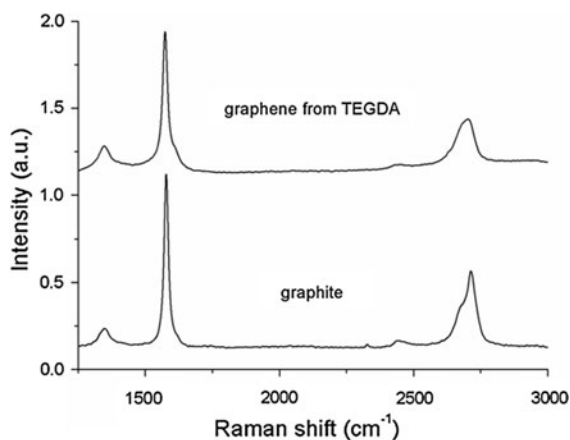these hardness measurements as the hardness value. SD was always below 2 %.

Results and discussion

As reported in the Introduction, some of the typical resins for dental and other biomedical applications are made of Bis-GMA/TEGDMA mixtures. Because of the higher dispersibility of graphene in TEGDA with respect to TEGDMA, since the structure of the two monomers is quite similar, we replaced TEGDMA with TEGDA in the copolymers with Bis-GMA.

Graphene dispersions in TEGDA with high nano-filler loadings were obtained by dispersing graphite flakes in TEGDA and subsequently ultrasonicating for allowing graphite exfoliation (Alzari et al. 2011b). This process has been explained in terms of solubility parameters on the basis of the favorable interactions of graphene flakes with the surrounding liquid matrix. In other words, the weak interactions (i.e., van der Waals forces, π interactions) among graphene flakes and monomer replace those present in graphite, responsible for graphene stacking, thus permitting the exfoliation (Coleman 2013).

By this method, in the present study graphene has been produced at high concentration in the monomer to be polymerized, with the great advantage of directly obtaining the corresponding nanocomposite.

The presence of few-layer graphene was confirmed by Raman spectroscopy (Fig. 1) and TEM analyses (not shown). As already observed in our previous article (Alzari et al. 2011b), the Raman spectra show the symmetric shape and position (2,703 cm^{-1}) of the 2D peak, typical of few-layer graphene (Ferrari et al. 2006) and differ from the graphite 2D peak (two components with a maximum at 2,713 cm^{-1}).

It is noteworthy that in this study, the maximum graphene concentration, as determined by gravimetry after filtration, was 6.00 mg ml^{-1}, which is one of the highest value reported so far (Nuvoli et al. 2011; Alzari et al. 2011a, b; Khan et al. 2011, 2010) in any solvent and by any graphene production method.

For this study, several copolymers (PBTs) made of Bis-GMA/TEGDA (constant ratio: 50:50 w/w), were prepared varying graphene concentration (from 0 to 0.270 wt%), by properly diluting a TEGDA masterbatch dispersion (graphene concentration: 6.00 mg ml^{-1}, Table 1).

Figure 2 shows the typical SEM micrographs of A3, A5 samples (both are graphene-filled) and of the corresponding neat polymer (sample A1). While the surface of the neat PBT appears completely smooth and homogeneous, it becomes as rougher as the graphene content increases. This finding can be explained by taking into account the strong interactions occurring between graphene and polymer matrix, which obstacle the straight propagation of the fracture that, otherwise, would result in a smooth surface. It is also worthy to note that a very homogeneous distribution of the graphene sheets within the polymer matrix is achieved for all the filled systems investigated, also including that characterized by the highest graphene content, as already reported in the literature (Alzari et al. 2011b).

In order to investigate the effect of graphene on the mechanical properties, hardness and compression tests were carried out on PBT copolymers containing different amounts of nanofiller, as listed above. Table 2

Fig. 1 Raman spectra of graphene obtained from dispersion of graphite in TEGDA compared with initial graphite

Table 1 Graphene concentration in the liquid dispersions and in the final nanocomposite materials

Sample	Graphene concentration in TEGDA (mg/ml)	Graphene concentration in PBT (wt%)
A1	0	0
A2	0.06	0.003
A3	0.24	0.011
A4	1.20	0.053
A5	6.00	0.270
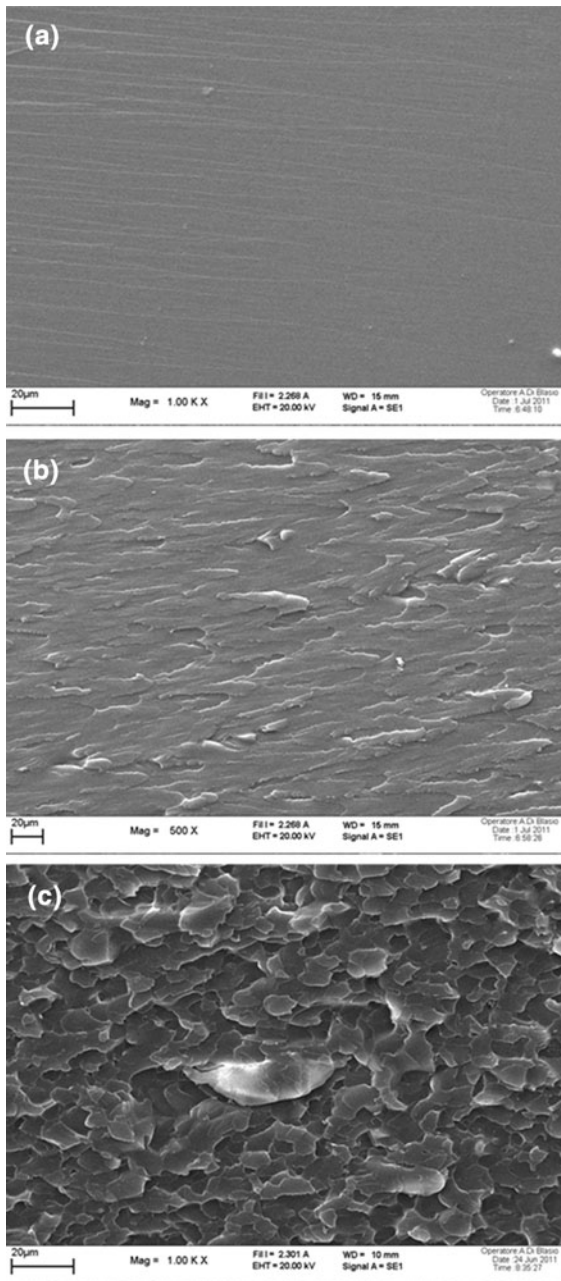
Fig. 2 SEM micrographs of Bis-GMA/TEGDA copolymers with different amounts of graphene: neat PBT (A1, **a**), 0.011 wt% (A3, **b**), and 0.270 wt% (A5, **c**)

Table 2 Hardness and modulus of elasticity for PBT filled with different amounts of graphene

Sample	Hardness—Shore A	Modulus of elasticity[a] (MPa)
R[b]	80	630 ± 22
A1	84	542 ± 16
A2	87	550 ± 13
A3	94	658 ± 19
A4	95	730 ± 29
A5	96	839 ± 15

[a] From compression tests

[b] Bis-GMA/TEGDMA (50/50)

Table 3 Degree of conversion and T_g values for PBT filled with different amounts of graphene

Sample	C %	T_g (°C)
R	97	46
A1	94	99
A2	94	99
A3	98	99
A4	95	99
A5	97	98

collects the obtained values of Shore A hardness and modulus of elasticity. For comparison, values referred to the unfilled resin prepared with TEGDMA instead of TEGDA are also presented (see R sample). First of all, a comparison between the neat polymer matrices was made. As can be seen in Table 2, Shore A hardness values indicate that the replacement of TEGDMA with TEGDA results in an increase of the hardness from 80 to 84. When graphene is embedded into the polymer matrix, the measured hardness turns out to depend on the nanofiller content; in particular, Shore A hardness increases up to 94 (12 % increase with respect to the unfilled PBT) for the sample containing 0.011 wt% graphene (sample A3), and to 96 (when the nanofiller concentration reaches 0.27 wt%; sample A5), thus indicating that hardness reaches a plateau in the presence of relatively low nanofiller amounts. This behavior can be ascribed to the formation of a percolated interphase region, occurring even at very low graphene concentrations, upon which the effect of the nanofiller on the thermal and mechanical properties is less pronounced (Ramanathan et al. 2008).

As far as compression tests are concerned, the replacement of TEGDMA with TEGDA worsens the compression strength, which, however, is compensated by the addition of the nanofiller. Indeed, graphene exerts a strong reinforcing effect on the polymer matrix even at very low concentration: the modulus of elasticity

increases with increasing graphene concentration, with a trend similar to that found for the hardness values.

DSC analyses were carried out to assess the degree of conversion (C %) and the glass transition temperature of PBT samples, which are listed in Table 3. For all samples, the degree of conversion was larger than 90 % regardless of the amount of graphene and the type of polymer matrix (i.e., TEGDMA- or TEGDA-based). At variance, the replacement of TEGDMA with TEGDA resulted in a significant T_g increase (from 46 to 99 °C for R and A1 samples, respectively). It is noteworthy that the presence of graphene does not influence the glass transition temperature (and therefore the crosslinking density of the cured network), which is stable around 99 °C. A similar behavior has been already assessed by other groups (Ansari and Giannelis 2009; Garboczi et al. 1995).

Conclusion

In this study, graphene has been used as reinforcing nanofiller in polymeric materials having potential applications for biomedical purposes. Bis-GMA/TEGDA has been chosen as polymer system because of its structure, which is similar to that of Bis-GMA/TEGDMA copolymer (widely used in the biomedical field); furthermore, TEGDA monomer is one of the best exfoliating media for graphene.

Graphene dispersions at high concentration were obtained by simple sonication in TEGDA monomer and directly used for synthesizing Bis-GMA/TEGDA nanocomposites. This synthetic strategy has significantly limited the reaggregation phenomena to graphite, which may occur during the nanofiller recovery in the solid-state. It should be also highlighted that graphene obtained directly by graphite exfoliation without any chemical manipulation looks to be a safe alternative (Hailong et al. 2010, Sasidharan et al. 2012, Vanesa et al. 2012) to other carbon forms, especially if compared with its oxidized forms (i.e., graphene oxide, or reduced graphene oxide), which are recognized as cytotoxic (Sasidharan et al. 2011, Sanchez et al. 2012).

The homogeneous dispersion of the nanofiller within the polymer matrix has been confirmed by SEM analyses, which showed rougher surfaces for all the nanocomposites with increased graphene concentration.

As far as the mechanical properties of the nanocomposites are concerned, graphene has been found to exert interesting reinforcing effects on the cured copolymers: indeed, both modulus of elasticity and surface hardness turned out to significantly increase even in the presence of small amounts of graphene. Finally, the glass transition temperature and hence the crosslinking density of the obtained nanocomposite networks were found to be substantially independent of the nanofiller content ($T_g \approx 99$ °C).

References

Aguilar MR, Elvira C, Gallardo A, Vázquez B, Román JS (2007) Smart polymers and their applications as biomaterials. In: Ashammakhi N, Reis R, Chiellini E (eds) Topics in tissue engineering vol 3. University of Oulu, Oulu, Finland

Aizawa T, Souda R, Otani S, Ishizawa Y, Oshima C (1990) Anomalous bond of monolayer graphite on transition-metal carbide surfaces. Phys Rev Lett 64:768–771

Alzari V, Nuvoli D, Scognamillo S, Piccinini M, Gioffredi E, Malucelli G, Marceddu S, Sechi M, Sanna V, Mariani A (2011a) Graphene-containing nanocomposite hydrogels of poly(N-isopropylacrylamide) prepared by frontal polymerization. J Mater Chem 21:8727–8733

Alzari V, Nuvoli D, Sanna R, Scognamillo S, Piccinini M, Kenny JM, Malucelli G, Mariani A (2011b) In situ production of high filler content graphene-based polymer nanocomposites by reactive processing. J Mater Chem 21:16544–16549

Ansari S, Giannelis EP (2009) Functionalized graphene sheet-poly(vinylidene fluoride) conductive nanocomposites. J Polym Sci Part B Polym Phys 47:888–897

Antonucci JM, Stansbury JW (1997) Molecular designed dental polymer. In: Arshady R (ed) Desk reference of functional polymers: synthesis and application. American Chemical Society, Publication, pp 719–738

Balandin AA, Ghosh S, Bao W, Calizo I, Teweldebrhan D, Miao F, Ning Lau C (2008) Superior thermal conductivity of single-layer graphene. Nano Lett 8:902–907

Ballo AM, Närhi TO, Akca EA, Ozenm T, Syrjänen SM, Lassila LVJ, Vallittu PK (2011) Prepolymerized vs. in situ-polymerized fiber-reinforced composite implants—a pilot study. J Dent Res 90:263–267

Berger C, Song Z, Li X, Wu X, Brown N, Naud C, Mayou D, Li T, Hass J, Marchenkov AN, Conrad EH, First PN, de Heer WA (2006) Electronic confinement and coherence in patterned epitaxial graphene. Science 312:1191–1196

Boukhvalov DW, Katsnelson MI (2008) Modeling of graphite oxide. J Am Chem Soc 130:10697–10701

Bowen RL (1962) Dental filling material comprising vinyl silane treated fused silica and a binder consisting of the reaction product of bisphenol and glycidyl acrylate. U.S. Patent 3066112

Bowen RL (1963) Properties of a silica-reinforced polymer for dental restorations. J Am Dent Assoc 66:57–64

Bowen RL (1965) Method of preparing a monomer having phenoxy and methacrylate groups linked by hydroxy glycerol groups. U.S. Patent 3179623

Chen M, Chen C, Hsu S, Sun SH, Su W (2005) Low shrinkage light curable nanocomposite for dental restorative material. Dent Mater 22:138–145

Coleman JN (2013) Liquid exfoliation of defect-free graphene. Acc Chem Res 46:14–22

Fan H, Wang L, Zhao K, Li N, Shi Z, Ge Z, Jin Z (2010) Fabrication, mechanical properties, and biocompatibility of graphene-reinforced chitosan composites. Biomacromolecules 11:2345–2351

Ferrari AC, Meyer JC, Scardaci V, Casiraghi C, Lazzeri M, Mauri F, Piscanec S, Jiang D, Novoselov KS, Roth S, Geim AK (2006) Quantifying defects in graphene via Raman spectroscopy at different excitation energies. Phys Rev Lett 97:187401–187403

Garboczi EJ, Snyder KA, Douglas JF, Thorpe MF (1995) Geometrical percolation-threshold of overlapping ellipsoids. Phys Rev E 52:819–828

Hernandez Y, Nicolosi V, Lotya M, Blighe FM, Sun Z, De S, McGovern IT, Holland B, Byrne M, Gun'ko YK, Boland JJ, Niraj P, Duesberg G, Krishnamurthy S, Goodhue R, Hutchison JH, Scardaci V, Ferrari AC, Coleman JN (2008) High-yeld production of graphene by liquid-phase exfoliation of graphite. Nat Nantechnol 3:563–568

Khan U, O'Neill A, Lotya M, De S, Coleman JN (2010) High-concentration solvent exfoliation of graphene. Small 6:864–871

Khan U, Porwal H, O'Neill A, Nawaz K, May P, Coleman JN (2011) Solvent-exfoliated graphene at extremely high concentration. Langmuir 27:9077–9082

Kim H, Abdala AA, Macosko CW (2010) Graphene/polymer. nanocomposites. Macromolecules 43:6515–6530

Lee C, Wei X, Kysar JW, Hone J (2008) Measurement of the elastic properties and intrinsic strength of monolayer graphene. Science 321:385–388

Lerf A, He H, Forster M, Klinowski J (1998) Structure of graphite oxide revisited. J Phys Chem B 102:4477–4482

Li X, Zhang G, Bai X, Sun X, Wang X, Wang E, Dai H (2008) Highly conducting graphene sheets and Langmuir-Blodgett films. Nat Nanotechnol 3:538–542

Lu X, Yu M, Huang H, Ruoff RS (1999) Tailoring graphite with the goal of achieving single sheets. Nanotechnology 10:269–272

Novoselov KS, Geim AK, Morozov SV, Jiang D, Zhang Y, Dubonos SV, Grigorieva IV, Firsov AA (2004) Electric field effect in atomically thin carbon films. Science 306:666–669

Novoselov KS, Geim AK, Morozov SV, Jiang D, Katsnelson MI, Grigorieva IV, Dubonos SV, Firsov AA (2005) Two-dimensional gas of massless Dirac fermions in graphene. Nature 438:197–200

Nuvoli D, Valentini L, Alzari V, Scognamillo S, Bittolo Bon S, Piccinini M, Illescas J, Mariani A (2011) High concentration few-layer graphene sheets obtained by liquid phase exfoliation of graphite in ionic liquid. J Mater Chem 21:3428–3431

Nuvoli D, Alzari V, Sanna R, Scognamillo S, Piccinini M, Peponi L, Kenny JM, Mriani A (2012) The production of concentrated dispersions of few-layer graphene by the direct exfoliation of graphite in organosilanes. Nanoscale Res Lett 7:674–680

Palussière J, Berge J, Gangi A, Cotten A, Pasco A, Bertagnoli R, Jaksche H, Carpeggiani P, Deramond H (2005) Clinical results of an open prospective study of a bis-GMA composite in percutaneous vertebral augmentation. Eur Spine J 14:982–991

Park S, Ruoff RS (2009) Chemical methods for the production of graphenes. Nat Nanotechnol 4:217–224

Ponomarenko L, Schedin F, Katsnelson MI, Yang R, Hill EW, Novoselov KS, Geim AK (2008) Chaotic Dirac billiard in graphene quantum dots. Science 320:356–358

Potts JR, Dreyer DR, Bielawski CW, Ruoff RS (2011) Graphene-based polymer nanocomposites. Polymer 52:5–25

Rafiee MA, Rafiee J, Wang Z, Song H, Yu ZZ, Koratkar N (2009) Enhanced mechanical properties of nanocomposites at low graphene content. ACS Nano 3:3884–3890

Ramanathan T, Abdala AA, Stankovich S, Dikin DA, Herrera-Alonso M, Piner RD, Adamson DH, Schniepp HC, Chen X, Ruoff RS, Nguyen ST, Aksay IA, Prud'Homme RK, Brinson LC (2008) Functionalized graphene sheets for polymer nanocomposites. Nat Nanotechnol 3:327–331

Roberson TM, Heyman H, Swift EJ (2002) Sturdevant's art and science of operative dentistry, 4th edn. Mosby Elsevier, St Louis

Sanchez VC, Jachak A, Hurt RH, Kane AB (2012) Biological interactions of graphene-family nanomaterials: an interdisciplinary review. Chem Res Toxicol 25:15–34

Sanna R, Sanna D, Alzari V, Nuvoli D, Scognamillo S, Piccinini M, Lazzari M, Gioffredi E, Malucelli G, Mariani A (2012) Synthesis and characterization of graphene-containing thermoresponsive nanocomposite hydrogels of poly(N-vinylcaprolactam) prepared by frontal polymerization. J Pol Sci Part A Polym Chem 50:4110–4118

Sasidharan A, Panchakarla LS, Chandran P, Menon D, Nair S, Rao CNR, Koyakutty M (2011) Differential nano-bio interactions and toxicity effects of pristine versus functionalized graphene. Nanoscale 3:2461–2464

Sasidharan A, Panchakarla LS, Chandran P, Menon D, Nair S, Rao CNR, Koyakutty M (2012) Graphene nanocomposite for biomedical applications: fabrication, antimicrobial and cytotoxic investigations. Nanotechnology 23:395101–395111

Schedin F, Geim AK, Morozov SV, Hill EW, Blake P, Katsnelson MI, Novoselov KS (2007) Detection of individual gas molecules adsorbed on graphene. Nat Mater 6:652–655

Scognamillo S, Gioffredi E, Piccinini M, Lazzari M, Alzari V, Nuvoli D, Sanna R, Piga D, Malucelli G, Mariani A (2012) Synthesis and characterization of nanocomposites of thermoplastic polyurethane with both graphene and graphene nanoribbon fillers. Polymer 53:4019–4024

Slonczewski JC, Weiss PR (1958) Band structure of graphite. Phys Rev 109:272–279

Sofo JO, Chaudhari AS, Barber GD (2007) Graphane: a two-dimensional hydrocarbon. Phys Rev B 75:153401–153404

Soh MS, Sellinger A, Yap AUJ (2006) Dental nanocomposites. Curr Nanosci 2:373–381

Stankovich S, Dikin DA, Dommett GHB, Kohlhaas KM, Zimney EJ, Stach EA, Piner RD, Nguyen ST, Ruoff RS (2006) Graphene-based composite materials. Nature 442:282–286

Stoller MD, Park S, Zhu Y, An J, Ruoff RS (2008) Graphene-based ultracapacitors. Nano Lett 8:3498–3502

Tuusa SM, Peltola MJ, Tirri T, Lassila LV, Vallittu PK (2007) Frontal bone defect repair with experimental glass-fiber-reinforced composite with bioactive glass granule coating. J Biomed Mater Res B Appl Biomater 82:149–155

Verdejo R, Barroso-Bujans F, Rodriguez-Perez MA, de Saja JA, Lopez-Manchado MA (2008) Functionalized graphene sheet filled silicone foam nanocomposites. J Mater Chem 18:2221–2226

Wang X, Zhi L, Müllen K (2008) Transparent, conductive graphene electrodes for dye-sensitized solar cells. Nano Lett 8:323–327

Wang X, Li X, Zhang L, Yoon Y, Weber PK, Wang H, Guo J, Dai H (2009) N-doping of graphene through electrothermal reactions with ammonia. Science 324:768–771

Yoo E, Kim J, Hosono E, Zhou H, Kudo T, Honma I (2008) Large reversible Li storage of graphene nanosheet families for use in rechargeable lithium ion batteries. Nano Lett 8:2277–2282

Zhao DS, Moritz N, Laurila P, Mattila R, Lassila LV, Strandberg N, Mäntylä T, Vallittu P, Aro HT (2009) Development of a multi-component fiber-reinforced composite implant for load-sharing conditions. Med Eng Phys 31:461–469